Synthesis, Structure, and Magnetic Properties of $CeNiIn_2$

Vasyl' I. Zaremba[a,b], Yaroslav M. Kalychak[a,b], Yuriy B. Tyvanchuk[b], Rolf-Dieter Hoffmann[a], Manfred H. Möller, and Rainer Pöttgen[a]

[a] Institut für Anorganische und Analytische Chemie, Westfälische Wilhelms-Universität Münster, Wilhelm-Klemm-Straße 8, 48149 Münster (Germany)
[b] Inorganic Chemistry Department, Ivan Franko National University of Lviv, Kyryla and Mephodiya Street 6, 79005 Lviv/Ukraine

Reprint requests to R. Pöttgen. E-mail: pottgen@uni-muenster.de

Z. Naturforsch. **57b,** 791–797 (2002); received April 22, 2002

Indium, Crystal Structure, Rare Earth Compound

Single crystals of the ternary indide $CeNiIn_2$ were synthesized from an indium flux. An arc-melted button of the starting composition $CeNiIn_2$ was annealed in a zirconia crucible with a slight excess of indium at 1200 K followed by slow cooling (5 K/h) to 870 K. The new indide has been investigated by X-ray diffraction on powders and single crystals: $PrNiIn_2$ type, *Cmcm*, $a = 440.78(4)$, $b = 1834.3(1)$, $c = 2178.8(2)$ pm, $wR2 = 0.0753$ for 1471 F^2 values and 66 variable parameters. The structure contains three crystallographically independent nickel positions which have a distorted trigonal prismatic coordination. The $CeNiIn_2$ structure is related to the $MgCuAl_2$ structure by chemical twinning. The shortest interatomic distances occur for Ni–In and In–In contacts. The nickel and indium atoms form a complex three-dimensional $[NiIn_2]$ network in which the cerium atoms fill distorted pentagonal channels. Magnetic susceptibility measurements indicate Curie-Weiss behavior with an experimental magnetic moment of 2.44(3) μ_B/Ce atom. At 3.4(3) K $CeNiIn_2$ orders ferro- or ferrimagnetically. The experimental saturation magnetization at 2 K and 5.5 T is 0.95(2) μ_B/Ce.

Introduction

The ternary systems rare earth metal (*RE*)-nickel-indium have attracted considerable interest in recent years with respect to their peculiar crystal structures and greatly varying physical properties [1, 2]. In the nickel rich regions of the phase diagrams, the structures often contain nickel clusters. An overview is given in reference [3]. With increasing indium content, Ni–In bonding plays a more dominant role and such structures are commonly composed of two- or three-dimensional $[Ni_xIn_y]$ polyanions [4, 5]. In the case of very indium rich compounds, one observes pronounced indium substructures with distorted indium centered In_8 cubes [3, 6, 7].

Several of the cerium, europium, gadolinium, and ytterbium containing indides have been studied with respect to their strong varying magnetic properties. To give some examples, CeNiIn [8–10], $YbNi_4In$, and $YbNiIn_4$ [11] show valence fluctuation, $Ce_5Ni_6In_{11}$ [12, 13] is a heavy fermion system, and GdNiIn is a 93.5 K ferromagnet [14].

Today more than 120 ternary intermetallic $RE_xNi_yIn_z$ compounds are known. The crystal chemistry and some properties have briefly been reviewed by Kalychak [2]. Each ternary system with lanthanum, cerium, praseodymium, and neodymium as rare earth metal component contains more than ten ternary indides. A precise investigation of the ternary systems (X-ray powder diffraction, metallography) at various temperatures is necessary for a detailed phase analysis. Our recent study of the cerium based system revealed the existence of the new intermetallic compound $CeNiIn_2$. The synthesis, structure determination, and the magnetic properties are reported herein.

Experimental Section

Synthesis

Starting materials for the preparation of $CeNiIn_2$ were cerium ingots (Johnson-Matthey), nickel wire (Johnson-Matthey, ∅ 0.38 mm), and indium tear drops (Johnson-Matthey), all with stated purities better than 99.9%. The cerium pieces were first arc-melted under argon (600 mbar) to small buttons and subsequently reacted with nickel wire and the indium tear drops with the starting composition 1:1:2. The resulting buttons were remelted three times to ensure homogeneity. The argon was first purified over molecu-

lar sieves, silica gel, and titanium sponge (900 K). Details about the arc-melting setup are given in reference [15].

After the arc-melting procedure, the crystals of $CeNiIn_2$ were very small and intergrown. We therefore decided to grow larger crystals in an indium flux. In the second step, a $CeNiIn_2$ button was placed in a zirconia crucible together with an excess of 10 weight-% indium. The zirconia crucible was covered with tantalum foil, sealed in an evacuated silica tube and rapidly heated to 1200 K. After 6 h the temperature was lowered by 5 K/h down to 870 K and the tube was quenched to room temperature by radiative heat loss. The sample could easily be separated from the zirconia crucible. No reaction with the crucible material was observed. After the slow cooling procedures large light gray crystalline fragments of $CeNiIn_2$ were formed. The excess indium flux remained at the top of the sample. $CeNiIn_2$ is stable in moist air. Fine-grain powders are dark gray; single crystals exhibit metallic luster.

EDX analyses

The sample was analyzed with a Leica 420 I scanning electron microscope using CeO_2, nickel, and InAs as standards. No metallic impurity elements were detected. Analyses of a well shaped single crystal (Fig. 1) revealed the composition 26 ± 1 at.-% Ce : 24 ± 1 at.-% Ni : 50 ± 1 at.-% In, close to the ideal composition.

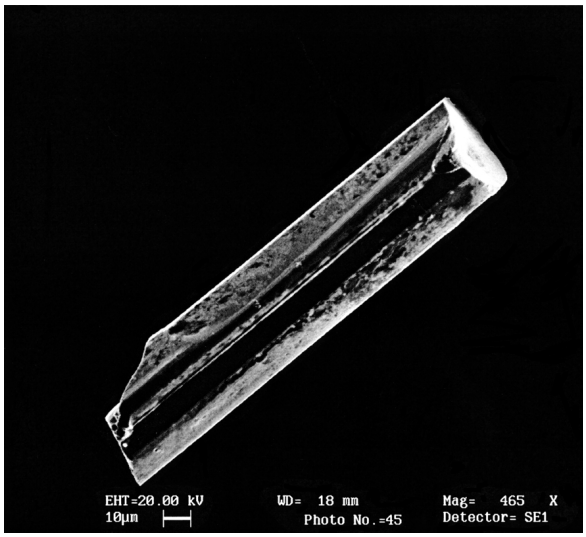

Fig. 1. Scanning electron micrograph of a $CeNiIn_2$ single crystal.

X-ray investigations

The sample was characterized through its Guinier powder pattern using Cu–K_{α_1} radiation and α-quartz (a = 491.30 pm, c = 540.46 pm) as an internal standard. The lattice parameters (Table 1) were obtained from least-squares fits of the powder data. To ensure correct indexing, the pattern was compared with a calculated one [16] taking the atomic positions from the structure refinement. The lattice parameters determined from the powder and the single crystal agreed well.

An irregularly shaped silvery single crystal of $CeNiIn_2$ was taken from the annealed sample. It was examined by Laue and rotation photographs on a RKV-86 camera with Mo–K radiation in order to establish suitability for intensity data collection. Single crystal intensity data were collected at r.t. by use of a four-circle diffractometer (CAD4) with graphite monochromatized Mo–K_α radiation (71.073 pm) and a scintillation counter with pulse height discrimination. The scans were performed in the $\omega/2\theta$ mode. An empirical absorption correction was applied on the basis of ψ-scan data. All relevant crystallographic data and experimental details for the data collection are listed in Table 1.

Table 1. Crystal data and structure refinement for $CeNiIn_2$.

Empirical formula	$CeNiIn_2$
Molar mass	428.47 g/mol
Unit cell dimensions	a = 440.78(4) pm
(Guinier powder data)	b = 1834.3(1) pm
	c = 2178.8(2) pm
	V = 0.1761 nm^3
Space group; Z	*Cmcm* (No. 63); Z = 20
Calculated density	8.08 g/cm^3
Crystal size	$25 \times 25 \times 80\ \mu m^3$
Transm. ratio (max/min)	1.81
Absorption coefficient	30.6 mm^{-1}
$F(000)$	3680
θ Range	2° to 30°
Range in hkl	+6, ±25, ±30
Total no. reflections	5648
Independent reflections	1471 (R_{int} = 0.0777)
Reflections with $I > 2\sigma(I)$	1082 (R_{sigma} = 0.0521)
Data/parameters	1471/66
Goodness-of-fit on F^2	1.036
Final R indices [$I > 2\sigma(I)$]	$R1$ = 0.0307
	$wR2$ = 0.0666
R Indices (all data)	$R1$ = 0.0574
	$wR2$ = 0.0753
Extinction coefficient	0.00027(2)
Largest diff. peak and hole	3.12 and −1.98 e/Å^3

Magnetic measurements

Temperature dependent magnetic susceptibility data of a 37.13 mg sample of $CeNiIn_2$ were determined with a MPMS SQUID magnetometer (Quantum Design) from 2 to 300 K with magnetic flux densities up to 5.5 T. The sample was enclosed in a silica tube and fixed at the sample holder rod. It was then cooled to 2 K in zero magnetic field and slowly heated to r.t. in an applied external field.

Structure refinement

The isotypism of $CeNiIn_2$ with the praseodymium compound [5] was already evident from the X-ray powder data. Consequently, analyses of the systematic extinctions led to space group *Cmcm*. The atomic parameters of $PrNiIn_2$ were taken as starting values and the structure was refined using SHELXL-97 (full-matrix least-squares on F_o^2) [17] with anisotropic atomic displacement parameters for all atoms. In a separate series of least-squares cycles we refined the occupancy parameters to check for deviations from the ideal composition. Since all sites were fully occupied within three standard deviations the ideal occupancies were assumed again in the final cycles. A final difference Fourier synthesis revealed no significant residual peaks (Table 1). The positional parameters and interatomic distances are listed in Tables 2 and 3. Listings of the observed and calculated structure factors are available.*

* Details may be obtained from: Fachinformationszentrum Karlsruhe, D-76344 Eggenstein-Leopoldshafen (Germany), by quoting the Registry No's. CSD-412515.

Table 3. Interatomic distances (pm), calculated with the lattice parameters taken from X-ray powder data of $CeNiIn_2$. All distances within the first coordination spheres are listed. Standard deviations are all equal or less than 0.3 pm.

Ce1:	1	Ni1	298.1	Ni2:	1	In5	265.4	In3:	1	Ni1	264.0
	2	Ni2	312.8		1	In6	267.5		2	Ni2	270.7
	1	In3	328.0		2	In3	270.7		2	In6	316.4
	2	In4	331.7		1	In4	279.5		2	In5	320.2
	2	In6	334.2		2	Ce3	309.4		2	Ce2	326.3
	2	In6	347.0		2	Ce1	312.8		1	In1	326.6
	2	In2	350.0						1	Ce1	328.0
	1	Ce3	375.7	Ni3:	2	In1	277.5		1	Ce3	331.1
	1	Ce2	396.2		1	Ce3	281.3				
					4	In4	287.3	In4:	1	Ni2	279.5
Ce2:	1	Ni3	310.9		2	Ce2	310.9		2	Ni3	287.3
	2	In3	326.3						1	In1	302.9
	2	In2	329.5	In1:	2	Ni3	277.5		1	In4	324.8
	2	Ni1	331.7		2	In4	302.9		2	Ce1	331.7
	1	In5	344.5		2	In5	305.2		1	In2	332.5
	2	In1	345.6		2	In3	326.6		2	Ce3	335.7
	2	In4	347.6		4	Ce2	345.6		2	Ce2	347.6
	1	In6	349.6								
	1	In2	354.1	In2:	1	Ni1	264.9	In5:	2	Ni2	265.4
	1	Ce1	396.2		2	Ni1	274.3		2	In1	305.2
					1	In6	294.0		4	In3	320.2
Ce3:	1	Ni3	281.3		2	In2	320.6		2	Ce3	337.8
	4	Ni2	309.5		2	Ce2	329.5		2	Ce2	344.6
	2	In3	331.1		1	In4	332.5				
	4	In4	335.6		2	Ce1	350.0	In6:	1	Ni2	267.5
	2	In5	337.8		1	Ce2	354.1		2	Ni1	274.7
	2	Ce1	375.7						1	In2	294.0
									1	In6	310.3
Ni1:	1	In3	264.0						2	In3	316.4
	1	In2	264.9						2	Ce1	334.2
	2	In2	274.3						2	Ce1	346.9
	2	In6	274.7						1	Ce2	349.6
	1	Ce1	298.1								
	2	Ce2	331.7								

Table 2. Atomic coordinates and anisotropic displacement parameters (pm^2) for $CeNiIn_2$. U_{eq} is defined as one third of the trace of the orthogonalized U_{ij} tensor. The anisotropic displacement factor exponent takes the form: $-2\pi^2[(ha^*)^2U_{11}+\ldots+2hka^*b^*U_{12}]$. $U_{12} = U_{13} = 0$.

Atom	Wyckoff position	*x*	*y*	*z*	U_{11}	U_{22}	U_{33}	U_{23}	U_{eq}
Ce1	8*f*	0	0.43745(4)	0.42021(4)	94(4)	69(3)	91(4)	14(2)	84(2)
Ce2	8*f*	0	0.22913(4)	0.37210(3)	69(4)	56(3)	95(3)	3(2)	74(2)
Ce3	4*c*	0	0.47018(6)	1/4	83(5)	62(5)	82(5)	0	76(2)
Ni1	8*f*	0	0.3443(1)	0.53234(8)	76(9)	81(8)	114(8)	–9(6)	90(3)
Ni2	8*f*	0	0.01524(9)	0.34220(8)	88(8)	78(8)	105(8)	1(6)	90(3)
Ni3	4*c*	0	0.3168(1)	1/4	85(13)	109(12)	196(14)	0	130(5)
In1	4*c*	0	0.72488(7)	1/4	96(6)	81(6)	99(6)	0	92(3)
In2	8*f*	0	0.80015(5)	0.46727(4)	84(4)	59(4)	102(4)	–15(3)	82(2)
In3	8*f*	0	0.59929(5)	0.35623(4)	82(5)	57(4)	101(4)	–14(3)	80(2)
In4	8*f*	0	0.86430(5)	0.32452(4)	87(5)	72(4)	101(4)	–3(3)	87(2)
In5	4*c*	0	0.10976(7)	1/4	96(7)	83(6)	96(6)	0	92(3)
In6	8*f*	0	0.06729(5)	0.45687(4)	87(5)	59(4)	90(4)	–7(3)	78(2)

Discussion

Crystal chemistry

$CeNiIn_2$ is a new indide and isotypic with the recently reported $RENiIn_2$ (*RE* = Pr, Nd, Sm). This peculiar structure type has first been refined for the praseodymium compound [5]. It seems to be limited to the larger rare earth elements as, in contrast, with the smaller rare earth metals Y, Eu, Gd–Dy, the $RENiIn_2$ indides crystallize with the $MgCuAl_2$ type structure [18, 19]. Both structure types are related *via* chemical twinning [20–24]. In Fig. 2 we present projections of the $CeNiIn_2$ and $GdNiIn_2$ structures (both space group *Cmcm*) onto the *bc* planes. The $CeNiIn_2$ structure may be considered as an intergrowth of $MgCuAl_2$ ($GdNiIn_2$) slabs. These slabs are connected at the mirror planes at *xy*1/4 and *xy*3/4 as emphasized by gray shading in Fig. 2.

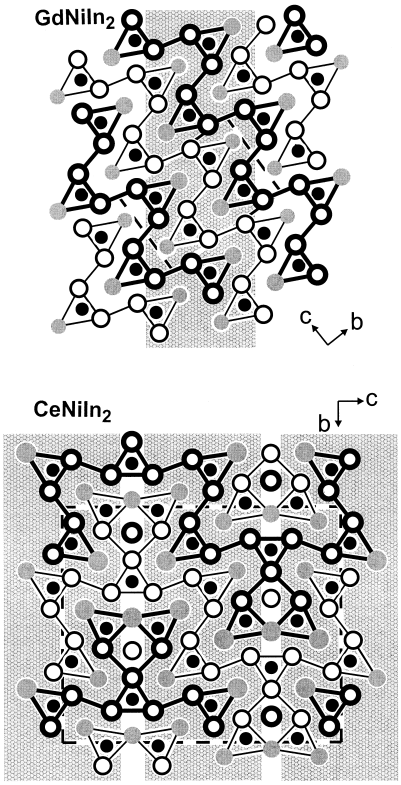

Fig. 2. Projection of the $CeNiIn_2$ and $GdNiIn_2$ structures along the short axes. The cerium (gadolinium), nickel, and indium atoms are drawn as gray, black, and open circles, respectively. All atoms lie on mirror planes at x = 0 (thin lines) and x = 1/2 (thick lines). The trigonal prismatic coordination of the nickel atoms and the similar structural slabs (gray shading) are emphasized.

In both structures the nickel atoms have a slightly distorted trigonal prismatic coordination. In $GdNiIn_2$ only one type of trigonal prisms occurs. Each nickel atom has two gadolinium and four indium neighbors. Due to the chemical twinning, three different trigonal prisms occur in the $CeNiIn_2$ structure. The Ni1 atoms have 2 Ce + 4 In neighbors, Ni2 has 4 Ce + 2 In and Ni3 has 6 In neighbors. In both structure types the prisms are capped by indium and cerium atoms on the rectangular faces leading to coordination number 9 for each nickel atom.

The various Ni–In distances in $CeNiIn_2$ range from 264 to 287 pm. Most of these distances are close to the sum of the covalent radii of 265 pm [25], indicating a dominant role of Ni–In bonding in this structure. The In–In contacts range from 294 to 333 pm. Most of these In–In distances are shorter than in the tetragonal body-centered structure of elemental indium (a = 325.2, c = 494.7 pm) [26], where each indium atom has four nearest neighbors at 325 pm and eight further neighbors at 338 pm. Thus, In–In bonding also is important in $CeNiIn_2$.

The indium substructure in $MgCuAl_2$ type compounds derives from the structure of hexagonal diamond, lonsdaleite [27–29]. This is no longer the case for the $PrNiIn_2$ type compounds. As a results of the chemical twinning we observe a higher degree of In–In connectivity. At the mirror planes at z = 1/4 and z = 3/4 the In5 atoms have a distorted cube like environment. These body-centered cubes have two cerium and six indium edges. This nearest-neighbor In–In coordination may be considered as a cutout of the elemental tetragonal body-centered indium structure [26]. Such cutouts have frequently been observed as structural fragments in various indium-rich indides [3, 6, 7].

In view of the strong Ni–In and In–In interactions, the $CeNiIn_2$ structure is best described by a three-dimensional $[NiIn_2]$ polyanion (Fig. 3) in which the cerium atoms fill distorted pentagonal channels. The cerium atoms show comparatively strong bonding to the $[NiIn_2]$ polyanion through relatively short Ce–Ni contacts, *i.e.* 298 pm Ce1–Ni1, 311 pm Ce2–Ni3, and even 281 pm Ce3–Ni3. The shorter distances compare well with the sum of the covalent radii of 280 pm [25].

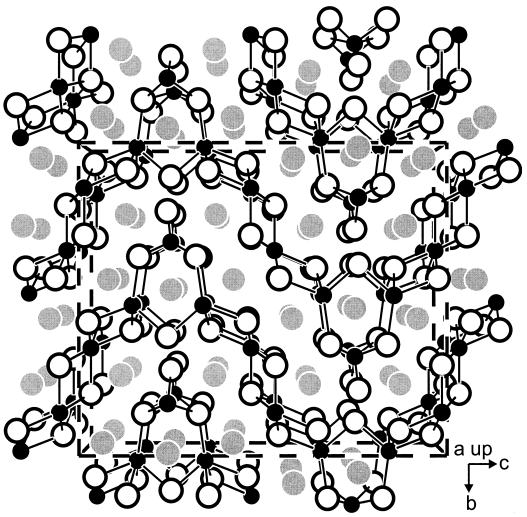

Fig. 3. Perspective view of the $CeNiIn_2$ structure along the *a* axis. The cerium, nickel, and indium atoms are drawn as gray, black, and open circles, respectively. The three-dimensional $[NiIn_2]$ network is emphasized.

A comparatively complex three-dimensional $[NiIn_4]$ polyanion occurs in the structure of $CeNiIn_4$ [4, 30]. The cerium atoms are also embedded in distorted pentagonal channels, however, the situation of chemical bonding is different. The main bonding features in the $[NiIn_4]$ polyanion are strong Ni–In and In–In contacts, but the shortest Ce–Ni distance of 342 pm is much longer than in $CeNiIn_2$. The shortest Ce–In distances in $CeNiIn_2$ and $CeNiIn_4$ are comparable. We can thus assume a much stronger bonding of the cerium atoms to the polyanion in $CeNiIn_2$ as compared with $CeNiIn_4$, although these structures have similar polyanions. The cerium atoms as the most electropositive component in $CeNiIn_2$ have largely transferred three valence electrons (see magnetic data below) to the nickel–indium network. In view of the strong Ni–In and In–In contacts, electron counting can to a first approximation, be written as $Ce^{3+}[NiIn_2]^{3-}$.

Finally we draw back to the range of existence for the $RENiIn_2$ intermetallics. With the larger rare earth metals cerium, praseodymium, neodymium, and samarium, the $PrNiIn_2$ type [5] occurs, while those indides with yttrium, europium, gadolinium, terbium, and dysprosium adopt the well known $MgCuAl_2$ structure [18]. At this point it is worthwhile to note that europium is divalent in $EuNiIn_2$ [19], and consequently the cell volume per formula unit of 89.6 Å^3 is even larger than that of $CeNiIn_2$ (87.9 Å^3). Based on these geometrical features one would expect the $PrNiIn_2$ structure also for the europium compound, however, the electronic structure might be different with a divalent rare earth metal. Samples with the large lanthanum atoms again show a different structure.

Magnetic properties

The temperature dependence of the inverse magnetic susceptibility of $CeNiIn_2$ is presented in Fig. 4. $CeNiIn_2$ shows Curie-Weiss behavior, but a slight convex curvature is observed for the $1/\chi$ *vs.* T plot, indicating a temperature-independent contribution. We have therefore fit the data above 40 K with a modified Curie-Weiss expression $\chi = \chi_0 + C/(T - \Theta)$ resulting in a paramagnetic Curie temperature (Weiss constant) of $\Theta = -9(1)$ K, an experimental magnetic moment of 2.44(3) μ_B/Ce, and a temperature independent contribution of = 0.00036(2) emu/mol. The experimental moment is close to the value of 2.54 μ_B for the free Ce^{3+} ion [31]. The temperature independent contribution is in the order of magnitude of a Pauli paramagnet and most likely results from the conduction electrons of this intermetallic compound.

At low temperature the susceptibility shows an anomaly indicative of ferro- or ferrimagnetic ordering. The exact Curie temperature was determined from a kink-point measurement (Fig. 5). The susceptibility was measured in a very low ex-

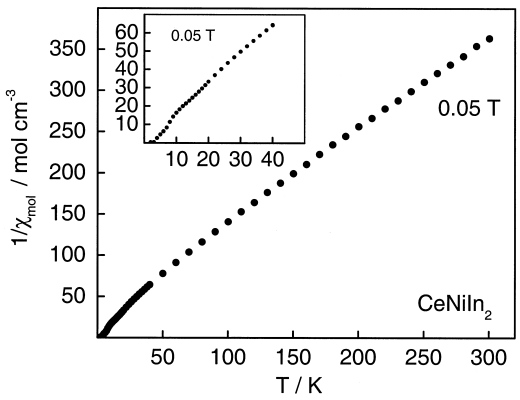

Fig. 4. Temperature dependence of the inverse magnetic susceptibility of $CeNiIn_2$, measured at a flux density of 0.05 T.

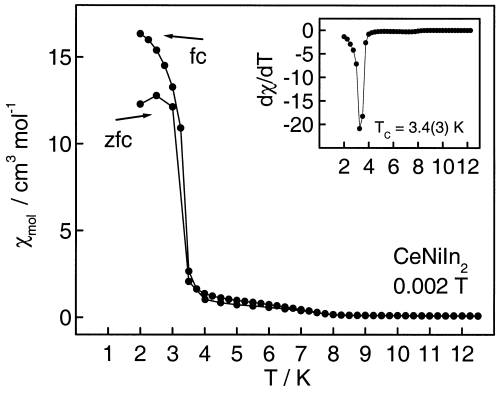

Fig. 5. Low-temperature susceptibility (zero field cooling and field cooling mode) of $CeNiIn_2$ at 0.002 T (kink-point measurement). The inset shows the derivative $d\chi/dT$ of the field cooling curve with a sharp peak at the Curie temperature of T_C = 3.4(3) K.

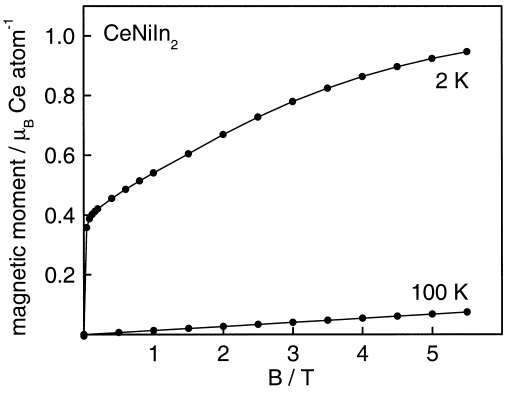

Fig. 6. Field dependence of the magnetic moment of $CeNiIn_2$ at 2 and 100 K.

ternal magnetic field of 0.002 T in zero field cooling and in field cooling mode. The derivative $d\chi/dT$ of the field cooling measurement resulted in a Curie temperature of T_C = 3.4(3) K. Also $CePdIn_2$ [32] with $MgCuAl_2$ type structure orders ferromagnetically, but at the higher Curie temperature of 10 K.

The magnetization data are plotted in Fig. 6. At 100 K, well above the magnetic ordering temperature, the magnetization isotherm is linear as expected for a paramagnetic compound. At 2 K the magnetization did not reach saturation at the highest obtainable field of 5.5 T. The magnetization at 2 K and 5.5 T is only 0.95(2) μ_B/Ce, significantly reduced from the theoretical one for Ce^{3+} of 2.14 μ_B/Ce [31]. Similar small moments have recently been observed for $CeRhSn_2$ [33], CeAuGe [34], and CePtSb [35]. These reduced moments are due to crystal field splitting of the J = 5/2 ground state of the Ce^{3+} ions.

Acknowledgments

We thank Dipl.-Ing. U. Ch. Rodewald for the intensity data collection and H.-J. Göcke for the work at the scanning electron microscope. This work was financially supported by the Fonds der Chemischen Industrie and by the Deutsche Forschungsgemeinschaft. V. I. Z. is indebted to the Alexander-von-Humboldt Foundation for a research stipend.

[1] P. Villars, L. D. Calvert, Pearson's Handbook of Crystallographic Data for Intermetallic Compounds, American Society for Metals, Materials Park, OH 44073, 2nd edn. 1991, and desk edition, 1997.
[2] Ya. M. Kalychak, J. Alloys Compd. **262–263,** 341 (1997).
[3] Ya. M. Kalychak, V. I. Zaremba, Ya. V. Galadzhun, Kh. Yu. Miliyanchuk, R.-D. Hoffmann, R. Pöttgen, Chem. Eur. J. **7,** 5343 (2001).
[4] R. Pöttgen, J. Mater. Chem. **5,** 769 (1995).
[5] V. I. Zaremba, Ya. M. Kalychak, V. P. Dubenskiy, R.-D. Hoffmann, R. Pöttgen, J. Solid State Chem. **152,** 560 (2000).
[6] R.-D. Hoffmann, R. Pöttgen, Chem. Eur. J. **6,** 600 (2000).
[7] R.-D. Hoffmann, R. Pöttgen, V. I. Zaremba, Ya. M. Kalychak, Z. Naturforsch. **55b,** 834 (2000).
[8] K. Satoh, T. Fujita, Y. Maeno, Y. Uwatoko, H. Fujii, J. Phys. Soc. Jpn. **59,** 692 (1990).
[9] M. Kurisu, T. Takabatake, H. Fujii, J. Magn. Magn. Mater. **90&91,** 469 (1990).
[10] H. Fujii, T. Takabatake, V. Andoh, J. Alloys Compd. **181,** 111 (1992).
[11] M. D. Koterlin, B. S. Morokhivskii, I. D. Shcherba, Ya. M. Kalychak, Phys. Solid State **41,** 1759 (1999).
[12] Ya. M. Kalychak, P. Yu. Zavalii, V. M. Baranyak, O. V. Dmytrakh, O. I. Bodak, Sov. Phys. Crystallogr. **32,** 600 (1987).
[13] J. Tang, K. A. Gschneidner (Jr.), S. J. White, M. R. Roser, T. J. Goodwin, L. R. Corrucini, Phys. Rev. B **52,** 7328 (1995).
[14] F. Merlo, M. L. Fornasini, S. Cirafici, F. Canepa, J. Alloys Compd. **267,** L12 (1998).
[15] R. Pöttgen, Th. Gulden, A. Simon, GIT-Laborfachzeitschrift **43,** 133 (1999).
[16] K. Yvon, W. Jeitschko, E. Parthé, J. Appl. Crystallogr. **10,** 73 (1977).
[17] G. M. Sheldrick, SHELXL-97, Program for Crystal Structure Refinement, University of Göttingen, Germany (1997).
[18] V. I. Zaremba, O. Ya. Zakharko, Ya. M. Kalychak, O. I. Bodak, Dopov. Akad. Nauk. Ukr. RSR, Ser. B 44 (1987).
[19] Ya. M. Kalychak, Ya. V. Galadzhun, Z. Kristallogr. **212,** 292 (1997).
[20] E. Parthé, B. Chabot, in: Handbook on the Physics and Chemistry of Rare Earths (K. A. Gschneidner (Jr.), L. Eyring, eds.), Vol. 6, p. 113, North-Holland, Amsterdam (1984).
[21] K. Cenzual, E. Parthé, Acta Crystallogr. Sect. C **40,** 1127 (1984).
[22] E. Parthé, B. Chabot, K. Cenzual, Chimia **39,** 164 (1985).
[23] E. Parthé, Elements of Inorganic Structural Chemistry, Pöge, Leipzig (1990).
[24] S. Andersson, Angew. Chem. **95,** 67 (1983).
[25] J. Emsley, The Elements, 3rd edn, Oxford University Press, Oxford (1999).
[26] J. Donohue, The Structures of the Elements, Wiley, New York (1974).
[27] R.-D. Hoffmann, U. Ch. Rodewald, R. Pöttgen, Z. Naturforsch. **54b,** 38 (1999).
[28] R.-D. Hoffmann, R. Pöttgen, Z. Anorg. Allg. Chem. **626,** 28 (2000).
[29] R.-D. Hoffmann, R. Pöttgen, Chem. Eur. J. **7,** 382 (2001).
[30] Ya. M. Kalychak, V. M. Baranyak, V. I. Zaremba, P. Yu. Zavalii , O. V. Dmytrakh and V. A. Bruskov, Sov. Phys. Crystallogr. **33**, 602 (1988).
[31] H. Lueken, Magnetochemie, Teubner, Stuttgart (1999).
[32] Y. Ijiri, F. J. DiSalvo, H. Yamane, J. Solid State Chem. **122,** 143 (1996).
[33] D. Niepmann, R. Pöttgen, B. Künnen, G. Kotzyba, C. Rosenhahn, B. D. Mosel, Chem. Mater. **11,** 1597 (1999).
[34] R. Pöttgen, H. Borrmann, R. K. Kremer, J. Magn. Magn. Mater. **152,** 196 (1996).
[35] B. D. Rainford, D. T. Adroja, Physica B **194–196,** 365 (1994).